



## Original Article

# Hill–Sachs lesion measurement with tridimensional models in anterior shoulder instability<sup>☆</sup>



Alberto Naoki Miyazaki, Luciana Andrade Silva\*, Pedro Doneux Santos, Guilherme do Val Sella, Leonardo Hideto Nagaya, Sergio Luiz Checchia

Grupo de Ombro e Cotovelo, Departamento de Ortopedia e Traumatologia, Faculdade de Ciências Médicas da Santa Casa de São Paulo, São Paulo, SP, Brazil

## ARTICLE INFO

## Article history:

Received 26 October 2016

Accepted 16 March 2017

Available online 4 April 2018

## Keywords:

Shoulder dislocation

Shoulder joint

Joint instability

Printing, three-dimensional printing

X-ray computed tomography

## ABSTRACT

**Objective:** To evaluate the reproducibility and repeatability of Hill–Sachs lesion measurement from computed tomography images, with computer software and tridimensional prototype.

**Methods:** Three-dimensional models were made from computed tomography images from 14 patients with anterior shoulder instability, using InVesalius 3.0<sup>®</sup> software. Hill–Sachs lesions were measured with Rhinoceros 5.0<sup>®</sup> software with pre-determined position. Mid-lateral distance, perpendicular to humeral shaft, cranial-caudal distance, parallel to humeral shaft, and the longitudinal distance of the lesion were measured. Using the Printer-ZP 310 three-dimensional printer, plaster models were made. To measure the Hill–Sachs lesion, a calibrated universal digital caliper was used in the same way as the software.

**Results:** There was intra-observer and inter-observer variability for measurement of the same model. Observers did not perform the measurements in a similar way, showing difficulty to use the method ( $p < 0.05$ ). Using the software to measure the mid-lateral distance, as well as in the measurement with the caliper, the model type influenced the measurements for each of the observers, rendering the method invalid ( $p < 0.05$ ).

**Conclusion:** There was no reproducibility and repeatability for Hill–Sachs lesion measurement between plaster models and software models.

© 2018 Sociedade Brasileira de Ortopedia e Traumatologia. Published by Elsevier Editora Ltda. This is an open access article under the CC BY-NC-ND license (<http://creativecommons.org/licenses/by-nc-nd/4.0/>).

<sup>☆</sup> Study conducted at Faculdade de Ciências Médicas da Santa Casa de São Paulo, Departamento de Ortopedia e Traumatologia, São Paulo, SP, with support of the Instituto Renato Archer, Campinas, SP, Brazil.

\* Corresponding author.

E-mails: [lucalu@terra.com.br](mailto:lucalu@terra.com.br), [ombro@ombro.med.br](mailto:ombro@ombro.med.br) (L.A. Silva).

<https://doi.org/10.1016/j.rboe.2018.03.008>

2255-4971/© 2018 Sociedade Brasileira de Ortopedia e Traumatologia. Published by Elsevier Editora Ltda. This is an open access article under the CC BY-NC-ND license (<http://creativecommons.org/licenses/by-nc-nd/4.0/>).

## Avaliação da mensuração da lesão de Hill-Sachs em modelos tridimensionais na luxação anterior de ombro

### R E S U M O

#### Palavras-chave:

Luxação do ombro  
Articulação do ombro  
Instabilidade articular  
Impressão tridimensional  
Tomografia computadorizada por raios X

**Objetivo:** Verificar se há reprodutibilidade e repetibilidade das mensurações diretas da lesão de Hill-Sachs (HS), a partir de imagens de reconstrução tomográficas, com o uso do programa de computador e em modelos obtidos por impressora tridimensional.

**Métodos:** Usaram-se imagens tomográficas de 14 pacientes com luxação recidivante do ombro feitas pelo serviço para construção dos modelos tridimensionais virtuais (*software InVesalius 3.0*<sup>®</sup>). Com o *software Rhinoceros 5.0*<sup>®</sup> mensurou-se a lesão de HS e padronizou-se uma posição para aferição das seguintes medidas: a maior distância mediolateral, perpendicular ao eixo da diáfise, a distância craniocaudal, paralela à diáfise, e a maior distância numa linha imaginária no eixo longitudinal da lesão. Com impressora tridimensional Printer-ZP 310 confeccionou-se os protótipos em gesso. Usou-se paquímetro digital universal calibrado, para fazer as três medidas da lesão de HS pré-estabelecidas. As mensurações foram feitas por aferição cega.

**Resultados:** Houve grande variabilidade intraobservador e interobservador para as medidas em uma mesma peça. Os observadores não fizeram as medições de forma similar, o que caracteriza a existência de dificuldade da mensuração pelo método ( $p < 0,05$ ). Nas mensurações no computador para aferição da distância mediolateral e na medição da peça com paquímetro, o tipo da peça influenciou a forma de feitura de medidas por cada um dos observadores, o que tornou o método de mensuração inválido ( $p < 0,05$ ).

**Conclusão:** Não houve reprodutibilidade e repetibilidade nas mensurações da lesão de HS, tanto em modelos de gesso quanto nas imagens de reconstrução tomográficas.

© 2018 Sociedade Brasileira de Ortopedia e Traumatologia. Publicado por Elsevier Editora Ltda. Este é um artigo Open Access sob uma licença CC BY-NC-ND (<http://creativecommons.org/licenses/by-nc-nd/4.0/>).

## Introduction

The Hill-Sachs (HS) lesion is very common and can be observed in almost 100% of patients with recurrent anterior shoulder dislocation.<sup>1</sup> This fracture occurs by compression of the posterolateral region of the humeral head against the anteroinferior portion of the glenoid during anterior dislocation of the shoulder, when the upper limb is abducted and laterally rotated.<sup>2</sup>

Burkhart and De Beer<sup>3</sup> have shown that in this position, depending on the size, the HS lesion creates a mechanism of engagement of the humeral head at the anterior edge of the glenoid, which would cause dislocation recurrence in 100% of cases. Other studies<sup>4,5</sup> have been conducted in this regard and, in 2014, Giacomo et al. introduced the concept of on-track and off-track, which would be an improvement of the original knowledge: in addition to the size of the lesion, its location and the bone loss of the glenoid would also be important factors in dislocation recurrence.<sup>6</sup> These authors present parameters and measurements to assess the size of the glenoid and of the HS lesion.

As early as 1984, Rowe et al.<sup>7</sup> created a classification that considered both the width and depth of the defect, based on the evaluation of axillary radiographs. Ito et al.<sup>8</sup> proposed new radiographic views. Flatow et al.<sup>9</sup> believed that the HS lesion was best assessed through direct visualization, which determines a percentage relationship between the size of the defect and the diameter of the humeral head. Three-dimensional

(3-D) reconstructions using computerized tomography are currently recommended to more accurately characterize HS lesions regarding their size, orientation, and morphology. With this type of examination, in 2014 Iyengar et al.<sup>10</sup> demonstrated that larger and more horizontal lesions tend to present a higher engagement. Other authors use software to measure the HS lesion from sagittal, coronal, and axial cuts, as well as from 3-D computed tomography reconstructions.<sup>11,12</sup> However, despite several methods were described for measuring the HS lesion, there is still no consensus as to how this measurement should be performed.

This study aimed to verify whether it is possible to measure the HS lesion using a computer, from tomographic reconstruction images, with a specific software and in a direct manner in models created with a 3-D printer; the study also sought to assess whether these measurements are reproducible and repeatable.

## Material and methods

For this experimental study, 14 patients with anterior recurrent shoulder dislocation followed-up at the Shoulder and Elbow Group were selected. All patients underwent the Latarjet procedure, which is the primary procedure. Only tomographic images of the patients made at this service and stored in Dicom format were used.

The images were inserted into the InVesalius 3.0<sup>®</sup> software, for the construction of virtual 3-D models. After

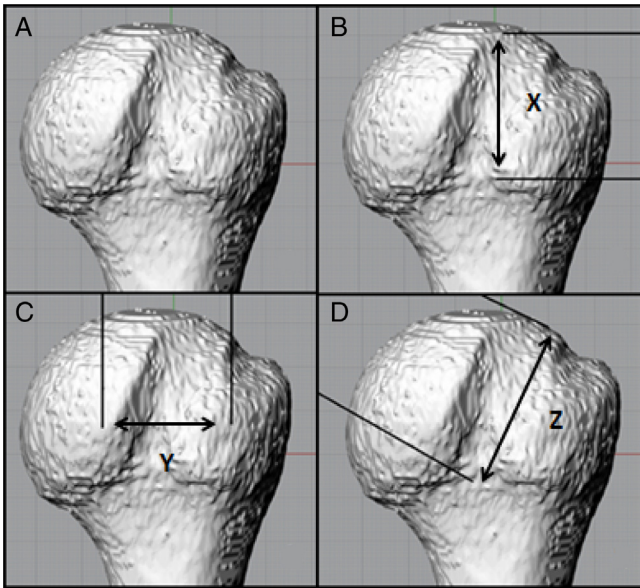


**Fig. 1 – A, three-dimensional reconstruction; B, measurement of the craniocaudal distance, represented by the letter X; C, measurement of the mediolateral distance, represented by the letter Y; D, measurement of the diagonal distance, represented by the letter Z.**

reconstruction, Rhinoceros 5.0<sup>®</sup> software was used to measure the HS lesion; for this purpose, a measuring position was standardized. This was determined based on objective anatomical points, so that it could be reproduced in all examinations: the posterior face of the humeral head when the intertubercular groove is at 45 degrees in the axial plane. Three measurements were made: the longest mediolateral distance of the lesion, perpendicular to the axis of the diaphysis; the craniocaudal distance, parallel to the axis of the diaphysis; and the longest distance in an imaginary line that followed the longitudinal axis of the lesion (Fig. 1).

The three-dimensional models were created from the tomographic images of the proximal humeral end using InVesalius 3.0<sup>®</sup> software. Using a Printer-ZP 310 3-D printer, the plaster prototypes were created, with precision between 0.1 mm and 0.2 mm (Fig. 2). Once the 3-D prototype was created, a calibrated universal digital caliper with a precision limit of 0.05 mm was used to measure the HS lesion, in accor-



**Fig. 2 – Three-dimensional plaster prototype.**

dance with the standard set for measurement in the software (Fig. 3). For both physical model and software, measurements were taken in three moments, with a six-week interval between them, by three observers (orthopedic shoulder surgeon) randomly selected in a draw made using Microsoft Excel 2010<sup>®</sup> software, which made the measurement blind.

For statistical analysis, the repeatability and reproducibility was assessed through analysis of variance, using the Minitab<sup>®</sup> software version 17, and the significance level was set at 5%.

For this study, the authors had the collaboration of the Information Technology Center, which provided the software InVesalius 3.0<sup>®</sup> and also the use of the printer for the 3-D models.

The study was approved by the Ethics Committee under No. 30533014.9.1001.5479.

## Results

Tables 1-3 present the values obtained in the three measurements, in random order, by the three observers. Data were submitted to statistical analysis, which proved a wide intra-observer and inter-observer variability for the measurements in the same model. Table 4 presents the *p*-values in relationship to the effects of the operator, the model, and the operator-model interaction. It also presents the percentage of the contribution of the measurement system variability to the total variability of the data, as well as the value obtained for

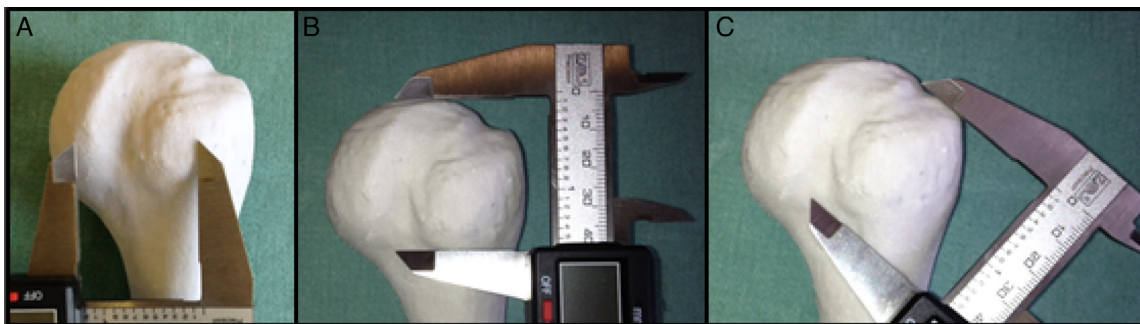


**Fig. 3 – A, measurement of the mediolateral distance with pachymeter; B, craniocaudal measurement with pachymeter; C, diagonal measurement with pachymeter.**

**Table 1 – Measurements, in millimeters, by the first observer.**

Round	Model	ML computer	CC computer	D computer	ML model	CC model	D model
1	1	28.51	17.27	27.06	28.4	18.04	26.78
1	2	21.17	26.61	35.7	17.81	29.9	38.4
1	3	14.37	24.57	24.23	18.78	20.45	28.03
1	4	27.23	31.17	35.2	25.43	34.98	40.32
1	5	20.51	26.54	31.03	17.12	31.05	32.51
1	6	23.29	27	33.49	23.4	29.97	31.55
1	7	21.17	25.89	25.85	9.04	18.51	15.72
1	8	20.46	32.04	32.6	20.68	37.06	40.98
1	9	14.45	27.61	26	12.39	25.81	31.85
1	10	18.6	33.19	36.11	15.84	31.24	37.97
1	11	18.6	27.75	28.41	17.31	35.35	40.44
1	12	20.31	28.61	26.36	5	12.23	20.26
1	13	12.51	17.03	16.18	7.77	19.01	22.27
1	14	19.6	35.5	36.59	16.71	33.21	34.52
2	1	28.97	18.42	28.02	22.82	24.28	29.52
2	2	20.03	27.75	34.72	18.33	28.43	39.78
2	3	17.27	22.94	24.5	19.93	24.07	28.33
2	4	26.77	31.98	34.94	24.86	34.83	37.96
2	5	23.64	27.69	30.22	8.39	16.44	16.57
2	6	23.87	27.93	34.26	22.57	28.18	38.22
2	7	10.59	21.03	20.27	6.95	17.47	15.87
2	8	20.49	25.08	28.47	20.3	19.03	39.06
2	9	15.31	28.32	33.27	8.35	16.86	15.73
2	10	16.59	30.47	37.1	16	33.3	36.23
2	11	18.45	25.03	26.06	11.87	29.99	16.03
2	12	18.02	28.32	30.34	2.69	13.98	16.3
2	13	11.59	9.44	9.01	7.4	19.35	21.11
2	14	18.6	34.19	33.41	20.62	34.98	32.51
3	1	27.2	18.97	26.54	28.25	23.63	28.35
3	2	19.43	27.79	34.84	17.16	33.66	37.56
3	3	19.49	22.51	22.89	21.43	13.76	13.64
3	4	24.81	30.02	34.22	25.61	35.34	37.68
3	5	16.36	25.33	28.15	16.45	26.11	27.68
3	6	22.51	25.43	27.06	22.64	27.1	30.66
3	7	10.68	20.84	19.69	9.37	17.98	17.7
3	8	21.62	31.52	29.92	22.11	36.47	40.45
3	9	16.08	27.14	29.14	14.15	30.33	31.95
3	10	17.76	29.85	35.76	16.84	28.88	33.93
3	11	10.17	27.54	28.54	12.22	29.95	15.48
3	12	15.4	16.73	18.39	4.75	15.27	21.06
3	13	10.53	17.3	18.7	6.23	21.4	23.67
3	14	17.89	33.2	33.31	16.94	32.7	50.64

Source: DOTSCMSP medical files.

CC computer, computer craniocaudal measurement; D computer, computer measurement at the axis of the lesion; ML computer, computer mediolateral measurement; CC model, craniocaudal measurement in the model; D model, axis of the lesion measurement in the model; ML model, mediolateral measurement in the model using a pachymeter.

the number of categories that the measurement system can distinguish.

In Table 4, regarding the model, it was observed that in the computer measurements of the mediolateral distance and in the model with pachymeter for the mediolateral distance, the model-operator interaction presented  $p < 0.05$ , indicating that the type of model influenced the way measurements were taken by each of the observers, making the measurement method invalid. In turn, the measurements for craniocaudal distance and the axis of the lesion made on the computer, in the model with a pachymeter for craniocaudal distance, and in the axis of the lesion in the model, the model-operator interaction presented  $p > 0.05$ , which indicates absence of the effect of this interaction (Table 4).

Regarding the observers, the  $p$ -value of the operator effect was  $p < 0.05$ , which demonstrates that the observers did not perform the measurements in a similar way, characterizing the difficulty of measurement by the method (Table 4).

In all cases, the percentage contribution of the variability was greater than 10%, indicating that none of the methods used were adequate (Table 4).

When assessing the different number of categories, which evaluates how a method can discriminate what is to be measured, ranging from one to five, this value was one in all measurements (except for the measurement of the mediolateral distance of the 3-D model with a pachymeter, which was valid to distinguish only two categories, since it presented

**Table 2 – Measurements, in millimeters, by the second observer.**

Round	Model	ML computer	CC computer	D computer	ML model	CC model	D model
1	1	26.67	23.67	27.72	26.52	21.41	29.21
1	2	30.18	33.76	36.08	19.9	33.7	39.55
1	3	16.02	23.89	25.22	23.59	23.81	28.83
1	4	27.75	34.62	38.48	29.49	36.53	37.99
1	5	18.37	30.91	33.64	23.59	35.9	38.25
1	6	13.6	22.55	26.68	27.49	31.36	36.48
1	7	14.61	23.33	25.28	13.13	20.04	13.15
1	8	21.17	27.47	27.8	25.21	32.97	40.45
1	9	27.75	34.62	38.48	16.83	30.91	32.93
1	10	18.88	31.76	37.34	18.46	32.55	38.42
1	11	11.3	26.49	28.5	16.03	30.3	32.9
1	12	26.38	34.1	31.83	9	16.54	21.56
1	13	12.72	14.66	16.69	16.66	20.27	28.98
1	14	21.59	40.15	42.44	19.9	35.85	39.62
2	1	28.16	21.55	27.76	24.63	27.87	32.82
2	2	21.46	33.9	35.88	18.74	26.33	37.75
2	3	22.36	30.48	31.5	28.13	22.49	30.63
2	4	27.23	34.3	36.48	28.76	37.79	39.11
2	5	18.19	26.14	34.7	22.23	32.38	39.08
2	6	25.03	34.07	38.77	26.81	31.83	35.23
2	7	19.31	29.61	28.6	13.51	26.26	27.84
2	8	23.14	33.38	31.2	32.19	40.4	41.88
2	9	24.91	38.93	42.19	17.13	27.17	31.36
2	10	28.9	37.19	41.66	19.97	32.47	37.69
2	11	26.54	40.56	42.88	15.22	26.8	33.89
2	12	22.43	35.32	33.06	16.24	24.69	26.55
2	13	14.31	13.16	11.9	20.73	18.99	26.76
2	14	18.75	35.54	36.14	18.81	35.65	39.92
3	1	15.22	25.85	28.27	25.15	29.35	23.2
3	2	19.56	30.88	33.33	18	27.16	36.36
3	3	17.09	24.49	31.21	24.69	24.66	29.11
3	4	26.99	30.85	34.88	28.14	38.93	40.01
3	5	18.03	26.68	31.37	19.79	35.26	33.53
3	6	25.54	30.12	32.71	26.81	34.01	29.91
3	7	12.48	17.11	17.68	12.52	19.83	21.27
3	8	22.52	33.71	32.07	31.87	41.68	37.03
3	9	18.14	33.33	38.9	17.98	33.27	29.34
3	10	22.78	35.77	38.36	17.8	23.81	18.36
3	11	17.37	30.88	32	13.42	32.74	31.13
3	12	23.16	33.58	33.67	7.54	22.5	12.28
3	13	16.68	25.54	28.02	15.53	37.77	29.46
3	14	19.43	35.13	37.53	19.88	27.72	34.02

Source: DOTSCMSP medical files.

CC computer, computer craniocaudal measurement; D computer, computer measurement at the axis of the lesion; ML computer, computer mediolateral measurement; CC model, craniocaudal measurement in the model; D model, axis of the lesion measurement in the model; ML model, mediolateral measurement in the model using a pachymeter.

value of 2). This indicates that the method used is not valid for any of the measurements (Table 4).

## Discussion

The studies by Burkhart and De Beer<sup>3</sup> in the 2000s rekindled the interest in the HS lesion, followed by the concept of glenoid track, or the “trail” that the glenoid makes on the humeral head during abduction and lateral rotation of the shoulder, as studied by Iyengar et al.<sup>10</sup> and Yamamoto et al.<sup>5</sup> This concept was extended in 2014 by Giacomo et al.,<sup>6</sup> in an article describing a method to determine whether a lesion would be on track or off track, and its correspondence with glenoid

edge injuries and lesion recurrence. In that specific study, the authors propose a method to measure the diameter of the glenoid and determine the size of the HS lesion, which are fundamental for the presented concepts to be applied and, thus, to guide the treatment of the recurrent anterior lesion. A more reliable assessment of the lesion may change the management of recurrent shoulder dislocations, with different treatment options for varying sizes of humeral head bone defects.<sup>2</sup>

All these studies highlight the importance of an accurate measurement of the HS lesion. Numerous authors have studied methods and exams to measure this lesion in the best way, from direct visualization to exams such as common radiographs, special views, or even computed tomography.

**Table 3 – Measurements, in millimeters, by the third observer.**

Round	Model	ML computer	CC computer	D computer	ML model	CC model	D model
1	1	15.41	30.71	33.43	25.44	27.02	32.27
1	2	22.75	31.76	36.64	21.45	32.99	39.81
1	3	20.74	30.94	29.75	21.27	28.4	35.27
1	4	28.39	34.41	37.9	28.44	36.08	40.14
1	5	23.64	32.1	34.74	21.09	33.14	37.32
1	6	27.35	32.91	37.2	27.3	31.81	39.1
1	7	13.88	26.32	28.19	10.45	22.6	23.5
1	8	22.61	33.73	37.2	25.83	38.03	40.52
1	9	15.41	33.72	37.14	18.11	34.06	35.05
1	10	22.6	33.62	37.25	21.68	37.71	40.56
1	11	18.31	33.62	34.52	11.15	28.19	32.73
1	12	14.61	34.67	35.59	10.16	16.38	20.08
1	13	10.8	15.3	17.26	8.95	19.23	23.93
1	14	20.84	35.68	38.94	24.11	36.05	40.79
2	1	17.15	32.1	35.02	18.3	23.71	28.33
2	2	20.86	31.29	34.36	21.76	36.39	40.03
2	3	16.11	33.95	34.21	21.89	24.58	27.89
2	4	26.3	34.53	34.13	28.9	33.85	37.93
2	5	22.02	35.92	37.23	21.78	30.93	35.87
2	6	29.47	31.76	37.62	24.04	30.43	35.63
2	7	12.01	20.31	21.75	9.52	18	17.89
2	8	22.08	38.32	36.15	22.62	36.07	40.2
2	9	14.66	37.44	41.38	14.53	31.65	34.62
2	10	20.46	36.48	39.49	16.05	30.73	33.12
2	11	11.44	32.9	31.93	14.15	29.79	34.36
2	12	10.44	34.76	39.74	6.96	17.44	19.71
2	13	8.69	21.67	30.02	9.55	21.66	21.55
2	14	20.06	40.34	41.65	20.59	32.14	39.46
3	1	30.12	20.74	29.88	22.33	21.06	26.23
3	2	20.33	35.13	34.35	18.58	32.73	34.9
3	3	15.7	27.54	28.2	22.23	27.08	27.82
3	4	28.66	31.06	34.89	24.56	33.86	35.69
3	5	26.99	33.98	40.19	20.58	33.3	34.74
3	6	27.52	31.68	32.07	24.53	28.42	37.71
3	7	12.22	27.02	27.89	7.56	15.55	15.84
3	8	22	35.13	34.35	19.05	36.66	38.55
3	9	16.21	32.68	40.46	11.98	31.61	32.4
3	10	19.63	33.45	36.34	19.14	31.57	36.42
3	11	13.9	29.72	30.65	12.04	28.46	35.09
3	12	7.15	17	18.19	5.15	12.65	15.51
3	13	9.01	12.48	16.47	13.36	22.63	23.21
3	14	18.14	35.39	37.01	21.5	35.59	38.8

Source: DOTSCMSP medical files.

CC computer, computer craniocaudal measurement; D computer, computer measurement at the axis of the lesion; ML computer, computer mediolateral measurement; CC model, craniocaudal measurement in the model; D model, axis of the lesion measurement in the model; ML model, mediolateral measurement in the model using a pachymeter.

**Table 4 – Assessment of repeatability and reproducibility using analysis of variance.**

	Model	Operator	Operator-model interaction	Contribution of the variability	Distinct number of categories
ML computer	$p < 0.05^a$	$p > 0.05^a$	$p < 0.05^a$	54.9%	1
CC computer	$p < 0.05^a$	$p < 0.05^a$	$p > 0.05^a$	43.98%	1
D computer	$p < 0.05^a$	$p < 0.05^a$	$p > 0.05^a$	41.43%	1
ML model	$p < 0.05^a$	$p < 0.05^a$	$p < 0.05^a$	25.43%	1
CC model	$p < 0.05^a$	$p < 0.05^a$	$p > 0.05^a$	36.1%	2
D model	$p < 0.05^a$	$p < 0.05^a$	$p > 0.05^a$	34.90%	1

Source: DOTSCMSP medical files.

CC computer, computer craniocaudal measurement; D computer, computer measurement at the axis of the lesion; ML computer, computer mediolateral measurement; CC model, craniocaudal measurement in the model; D model, axis of the lesion measurement in the model; ML model, mediolateral measurement in the model using a pachymeter;  $p$ ,  $p$ -value.

<sup>a</sup> ANOVA.

In 2011, Cho et al.<sup>4</sup> measured HS lesions from 2-D computed tomography images as well as 3-D images to determine the location and orientation of the lesion. The measurements, made by two observers following the proposed method, presented repeatability and reproducibility. However, the statistical method known as linearity coefficient was used, as the selected images already had a certain pre-determination of the points for their measurement. This may have created a bias in the study.

In the same year, Kodali et al.<sup>12</sup> created HS lesions in physical models and generated computed tomography images, which were evaluated two-dimensionally for size and depth. In the 2-D measurement, they were able to measure the depth correctly; however, the width of the lesion was always underestimated. The authors proposed that this assessment could be performed three-dimensionally. The study by Iyengar et al.<sup>10</sup> determined that 3-D computed tomography reconstruction of the HS lesion is the gold standard for determining its volume.

The present authors believed that, in real plaster models created using a 3-D printer after 3-D computerized reconstruction, it would be easy to measure HS lesions and then verify whether these measurements would be in accordance with those made in a computer. To avoid bias in the position where each CT was taken, the shoulder cut position was standardized: through the bicipital groove, an objective point relative to the axial plane. Therefore, all 14 humeral heads were in the same position when the lesion was measured.

However, to the authors' surprise, both the measurements of the plaster model under direct vision and using the computer demonstrated that the method did not present reproducibility and repeatability in the measurements. The authors believe that both intra-observer and inter-observer variation existed in both methods; due to the subjectivity and imprecision regarding the limits of the injury, the same observer could change the point to be measured in the same model at different times, which was evidenced by the results presented by the three observers responsible for measurement in the present study.

Therefore, the HS lesion could not be measured with the desired precision. Both *in vivo* and on the computer, the definition of the points that allow this measurement is quite difficult even for experienced shoulder surgeons, who are used to assessing preoperative computed tomography scans and defining the treatment of recurrent anterior lesions. The authors believe that there is still much to study in this area, and that it is necessary to develop other methods to assess the exact size of the HS lesion.

## Conclusion

The measurements of the HS lesion did not present reproducibility or repeatability, both in the 3-D plaster models and

in the 3-D computerized images obtained from the tomographic images.

A reliable and reproducible method for assessing the HS lesion is still required.

## Conflicts of interest

The authors declare no conflicts of interest.

## REFERENCES

- Hill HA, Sachs MD. The grooved defect of the humeral head: a frequently unrecognized complication of dislocations of the shoulder joint. *Radiology*. 1940;35:690-700.
- Chen LA, Hunt SA, Hawkins RJ, Zuckerman JD. Management of bone loss associated with recurrent anterior glenohumeral instability. *Am J Sports Med*. 2005;33(6):912-24.
- Burkhart SS, De Beer JF. Traumatic glenohumeral bone defects and their relationship to failure of arthroscopic Bankart repairs: significance of the inverted-pear glenoid and the humeral engaging Hill-Sachs lesion. *Arthroscopy*. 2000;16(7):677-94.
- Cho SH, Cho NS, Rhee YG. Preoperative analysis of the Hill-Sachs lesion in anterior shoulder instability. *Am J Sports Med*. 2011;39(11):2389-95.
- Yamamoto N, Itoi E, Abe H, Minagawa H, Seki N, Shimada Y, et al. Contact between the glenoid and the humeral head in abduction, external rotation, and horizontal extension: a new concept of glenoid track. *J Shoulder Elbow Surg*. 2007;16(5):649-56.
- Giacomo DG, Itoi E, Burkhart SS. Evolving concept of bipolar bone loss and the Hill-Sachs lesion: from "engaging/non-engaging" lesion to "on-track/off track" lesion. *Arthroscopy*. 2014;30(1):90-8.
- Rowe CR, Zarins B, Ciuillo JV. Recurrent anterior dislocation of the shoulder after surgical repair: apparent causes of failure and treatment. *J Bone Joint Surg Am*. 1984;66(2):159-68.
- Ito H, Takayama A, Shirai Y. Radiographic evaluation of the Hill-Sachs lesion in patients with recurrent anterior shoulder instability. *J Shoulder Elbow Surg*. 2000;9(6):495-7.
- Flatow EL, Warner JJ. Instability of the shoulder: complex problems and failed repairs. Part I: relevant biomechanics, multidirectional instability, and severe glenoid loss. *Instr Course Lect*. 1998;47:97-112.
- Iyengar JJ, Jiang KN, Kwon D, Lustbader EG, Ahmad CS. 3-D modeling of humeral head defects in glenohumeral instability: clinical implications of lesion morphology and the glenoid track. *J Shoulder Elbow Surg*. 2014;23(9):e230-1.
- Saito H, Itoi E, Minagawa H, Yamamoto N, Tuoheti Y, Seki N, et al. Location of the Hill-Sachs lesion in shoulders with recurrent anterior dislocation. *Arch Orthop Trauma Surg*. 2009;129(10):1327-34.
- Kodali P, Jones MH, Polster J, Miniaci A, Fening SD. Accuracy of measurement of Hill-Sachs lesions with computed tomography. *J Shoulder Elbow Surg*. 2011;20(8):1328-34.